DTIC FILE COPY

(2)

MECH-119

AD-A197 194

TOUGHENING BY ALIGNED, FRICTIONALLY CONSTRAINED FIBERS

DTIC
ELECTE
JUL 2 6 1988
S D
H

BERNARD BUDIANSKY and JOHN C. AMAZIGO

Division of Applied Sciences
HARVARD UNIVERSITY
Cambridge, Massachusetts 02138

883191

March 1988

DISTRIBUTION STATEMENT A
Approved for public release;
Distribution Unlimited

TOUGHENING BY ALIGNED, FRICTIONALLY CONSTRAINED FIBERS

BERNARD BUDIANSKY and JOHN C. AMAZIGO*
DIVISION OF APPLIED SCIENCES
HARVARD UNIVERSITY
CAMBRIDGE, MA 02138

March 1988

ABSTRACT

The Mode-I fracture toughness of a brittle material reinforced by aligned brittle fibers is studied theoretically. The fibers are assumed to slip relative to the matrix when a critical interface shear stress is reached, and the toughening action of the fibers is presumed to be due to bridging of crack faces in the vicinity of the crack front. The toughening due to the fiber reinforcement is related to basic parameters associated with the related problem of steady-state matrix cracking in the presence of intact fibers. Bridge lengths at fracture and fracture resistance curves are calculated.

NOMENCLATURE

a	fiber radius
c	fiber volume fraction
E	longitudinal composite Young's modulus, $\approx cE_f + (1-c)E_m$
E_f, E_m	fiber, matrix Young's moduli
G_f, G_m	fiber, matrix shear moduli
$\mathcal{G}_m$	critical matrix energy-release-rate, $= (1-\nu^2_m)K^2_m/E_m$
K	applied stress-intensity factor
K_m	critical matrix stress-intensity factor
L	bridge length
Q	complementary energy, spring model
S	fiber breaking stress
V	strain energy, spring model
v	crack-face displacement
α	non-dimensional bridge length, Eq. (26)
Λ	modified toughening ratio, Eq. (19)

* On leave from the Department of Mathematics, University of Nigeria, Nsukka, Nigeria.

λ	toughening ratio, K/K_m
ν_f, ν_m	fiber, matrix Poisson's ratio
σ_0, σ_1	reference stresses, Eqs. (1-2)
σ_{cr}	critical stress, steady-state matrix cracking
τ	fiber-matrix interface shear resistance

INTRODUCTION

This paper addresses the problem of calculating the increase in the Mode I, plane-strain fracture toughness of a brittle material when it is reinforced by long, aligned, brittle fibers, with sliding between the fibers and the matrix suppressed only if the interface frictional shear is less than some limiting stress. The configuration contemplated (Fig. 1) is an infinite domain containing a semi-infinite crack that is bridged by intact fibers in the vicinity of the crack tip. The crack is growing in a quasi-static, steady-state fashion, with simultaneous fracture of the matrix along the crack front and failure of the fibers at the end of the bridged zone. This crack propagation is imagined to occur under the imposition of a remote stress field that corresponds to an "applied" stress concentration factor K, which is accordingly defined as the fracture toughness of the composite material. The primary aim of the present study is to provide theoretical results for the *toughening ratio* $\lambda = K/K_m$, where K_m is the fracture toughness of the unreinforced matrix material. In addition, resistance curves will be produced, showing how an initially unbridged crack grows into the matrix material as the applied K is increased towards its critical value.

The present results should be applicable to less idealized geometries if the conditions of *small-scale bridging* are met, wherein the bridge length L is small relative to all other pertinent dimensions, such as crack length and distance of the crack tip from the boundary. Work on the toughening problem by MARSHALL and EVANS (1986) and MARSHALL and COX (1987) considered configurations for which the small-scale assumption was not made. Besides its emphasis on small-scale bridging, the present paper differs from these studies primarily in the way the analysis and results are linked closely to basic parameters associated with steady-state matrix cracking *without* fiber failure (BUDIANSKY, HUTCHINSON, and EVANS, 1986). The importance of a statistical variation in fiber strength have recently been emphasized by THOULESS and EVANS (1988), and the influence of residual stresses has been discussed by MARSHALL and EVANS (1988), but these effects are not considered in the present paper, which is based upon the preliminary analysis that was outlined by BUDIANSKY (1986).

STEADY-STATE MATRIX CRACKING

We review here results found by BUDIANSKY, HUTCHINSON, and EVANS (BHE) for the stress σ_{cr} associated with steady matrix cracking (Fig. 2). In the absence of initial stresses, σ_{cr} is given in Fig. 3 in terms of the reference stresses σ_0 and σ_1 defined by

$$\sigma_0/E = B\left[\frac{6c^2E_f}{(1-c)^2E(1+\nu_m)}\right]^{1/4}\left[\frac{G_m}{aE_m}\right]^{1/2} \tag{1}$$

and

$$\sigma_1/E = \left[\frac{6c^2E_f\tau}{(1-c)EE_m}\right]^{1/3}\left[\frac{G_m}{aE_m}\right]^{1/3} \tag{2}$$

where

$$B = \left[\frac{2(1-c)^3}{-6\log c - 3(1-c)(3-c)}\right]^{1/4} \tag{3}$$

The ratio σ_1/σ_0 plays a key role as a non-dimensional parameter that characterizes the frictional shear strength of the fiber-matrix interface. For $\tau \to 0$, $\sigma_1/\sigma_0 \to 0$, and then $\sigma_{cr} \to \sigma_1$; thus, σ_1 is the critical stress for matrix cracking when there is extensive interface slip between the matrix and the bridging fibers. On the other hand, for $\sigma_1/\sigma_0 > 3^{1/3}$ there is no interface slip during steady-state matrix cracking, and in this case $\sigma_{cr} = \sigma_0$.

For $\sigma_1/\sigma_0 < 3^{1/3}$, the curve in Fig. 3 was described parametrically in BHE by

$$\frac{\sigma_{cr}}{\sigma_0} = \frac{Y}{3}\left(\frac{\sigma_1}{\sigma_0}\right)^3 , \qquad \frac{\sigma_1}{\sigma_0} = \left(\frac{27}{Y^3+3Y-1}\right)^{1/6} \tag{4}$$

for $1 < Y < \infty$. This provides the implicit equation

$$\left(\frac{\sigma_{cr}}{\sigma_1}\right)^3 + \frac{1}{3}\left(\frac{\sigma_{cr}}{\sigma_1}\right)\left(\frac{\sigma_1}{\sigma_0}\right)^4 - \frac{1}{27}\left(\frac{\sigma_1}{\sigma_0}\right)^6 = 1 \tag{5}$$

for σ_{cr}.

If the fibers remain intact after the matrix is fully cracked, the composite may continue to resist additional stress, as shown schematically by the idealized stress-strain relation in Fig. 4. The ultimate composite strength is then approximately $\sigma_{max} = cS$, where S is the breaking stress of the fibers.

For
Distribution/
Availability Codes
Avail and/or
Dist Special
A-1
DTIC
COPY
INSPECTED

SPRING MODEL; EQUIVALENT NONLINEAR SPRING STIFFNESS

The steady-state matrix cracking problem of Fig. 2 may be modeled by the configuration shown in Fig. 5a, wherein crack-bridging springs of zero initial length are imagined to emerge continuously from the crack tip as the crack grows. The stress σ in the springs will be assumed to depend on the the crack opening δ=2v (Fig. 6) in such a way as to make the matrix cracking stress of the model the same as that of the fibrous composite. In establishing this equivalence, the crack-tip energy-release-rate G_m in the model problem will be modified by the factor (1-c) in order to simulate the reduction in crack area associated with the presence of fibers. Once the appropriate spring characteristics are thereby deduced from the BHE results for steady-state matrix cracking, we will be able to use the spring model to study the toughening problem (Fig. 1).

By setting the modified crack-tip energy-release-rate equal to the difference between the far upstream and downstream potential energies per unit length, we get the condition

$$\sigma_{cr}\delta(\sigma_{cr}) - \int_0^{\sigma_{cr}} \sigma d\delta = (1-c)G_m \tag{6}$$

governing the critical matrix-cracking stress of the model problem. Alternatively, we can write the J-integral (RICE, 1968)

$$J = \int_\Gamma \left[\int_0^{\sigma_{\alpha\beta}} \sigma_{\alpha\beta} d\varepsilon_{\alpha\beta} n_x - \sigma_{\alpha\beta} \frac{\partial u_\beta}{\partial x} n_\alpha \right] ds = 0 \tag{7}$$

around the path shown in Fig. 5b to get the same result, if, again, we multiply the contribution from the small circle around the crack tip by the factor (1-c). Eq. (6) is equivalent to

$$\frac{Q(\sigma_{cr})}{(1-c)G_m} = 1 \tag{8}$$

where (see Fig. 6) Q is the *complementary energy* function

$$Q(\sigma) = \int_0^{\sigma} \delta d\sigma \,. \tag{9}$$

Note, for future reference, that the *strain energy*

$$V(\sigma) = \int_0^{\sigma} \sigma d\delta \tag{10}$$

is related to $Q(\sigma)$ by

$$V(\sigma) = \sigma Q'(\sigma) - Q(\sigma). \tag{11}$$

We now demand that the cracking criterion (8) give the BHE results for σ_{cr}. In the slipping-fiber case, we equate the left-hand sides of (5) and (8) to get

$$\frac{Q(\sigma_{cr})}{(1-c)G_m} = \left(\frac{\sigma_{cr}}{\sigma_1}\right)^3 + \frac{1}{3}\left(\frac{\sigma_{cr}}{\sigma_1}\right)\left(\frac{\sigma_1}{\sigma_0}\right)^4 - \frac{1}{27}\left(\frac{\sigma_1}{\sigma_0}\right)^6. \tag{12}$$

In the no-slip case, the cracking criterion may be written as $(\sigma_{cr}/\sigma_0)^2 = 1$, and comparison of this with (8) gives

$$\frac{Q(\sigma_{cr})}{(1-c)G_m} = \left(\frac{\sigma_{cr}}{\sigma_0}\right)^2. \tag{13}$$

(The validity of these identifications is corroborated by the fact that the right-hand sides of both (12) and (13) are indeed proportional to $1/G_m$.) We can now write a general formula for $Q(\sigma)$ by noting that the no-slip condition for fibers (Eq. (27) of BHE) may be expressed as

$$\frac{\sigma}{\sigma_0} \le \frac{1}{3}\left(\frac{\sigma_1}{\sigma_0}\right)^3 \tag{14}$$

in terms of the smeared-out fiber stresses σ at the crack face. Accordingly, the complementary energy function for the springs is

$$Q(\sigma) = \left(\frac{\sigma}{\sigma_0}\right)^2 (1-c)G_m \qquad \text{for } \frac{\sigma}{\sigma_0} \le \frac{1}{3}\left(\frac{\sigma_1}{\sigma_0}\right)^3 \tag{15a}$$

$$= \left[\left(\frac{\sigma}{\sigma_1}\right)^3 + \frac{1}{3}\frac{\sigma}{\sigma_1}\left(\frac{\sigma_1}{\sigma_0}\right)^4 - \frac{1}{27}\left(\frac{\sigma_1}{\sigma_0}\right)^6\right](1-c)G_m \qquad \text{for } \frac{\sigma}{\sigma_0} \ge \frac{1}{3}\left(\frac{\sigma_1}{\sigma_0}\right)^3. \tag{15b}$$

From (11), the strain energy function is

$$V(\sigma) = \left(\frac{\sigma}{\sigma_0}\right)^2 (1-c)G_m \qquad \text{for } \frac{\sigma}{\sigma_0} \le \frac{1}{3}\left(\frac{\sigma_1}{\sigma_0}\right)^3 \tag{16a}$$

$$= \left[2\left(\frac{\sigma}{\sigma_1}\right)^3 + \frac{1}{27}\left(\frac{\sigma_1}{\sigma_0}\right)^6\right](1-c)G_m \qquad \text{for } \frac{\sigma}{\sigma_0} \ge \frac{1}{3}\left(\frac{\sigma_1}{\sigma_0}\right)^3. \tag{16b}$$

(This last equation for V corrects errors in Eq. (28) of BUDIANSKY (1986)). Finally, the stress-displacement relation for the springs is given by $v = \delta/2 = Q'(\sigma)/2$, whence

$$v = \left(\frac{\sigma}{\sigma_0^2}\right)(1-c)G_m \qquad \text{for } \frac{\sigma}{\sigma_0} \le \frac{1}{3}\left(\frac{\sigma_1}{\sigma_0}\right)^3 \tag{17a}$$

$$= \left[\frac{3}{2}\frac{\sigma^2}{\sigma_i^3} + \frac{1}{6}\frac{\sigma_1^3}{\sigma_0^4}\right](1-c)G_m \qquad \text{for } \frac{\sigma}{\sigma_0} \ge \frac{1}{3}\left(\frac{\sigma_1}{\sigma_0}\right)^3 . \tag{17b}$$

FRACTURE TOUGHNESS

We now contemplate the configuration in Fig. 1, and model it with that shown in Fig. 7a, wherein the semi-infinite crack is partially bridged by springs possessing the properties that we have just established. Far from the crack tip the material is regarded as homogeneous but orthotropic, and subjected to the far-field stress state

$$\sigma_{\alpha\beta} = \frac{K}{\sqrt{2\pi r}} f_{\alpha\beta}(\theta) \tag{17}$$

where $f_{\alpha\beta}(0) = 1$, and the angular distribution function $f_{\alpha\beta}(\theta) = f_{\alpha\beta}(-\theta)$ is appropriate for the particular orthotropy of the composite. Thus K is an "applied" Mode-I stress-intensity factor, while the stress-intensity factor along the crack edge in the matrix material is assumed equal to K_m. Now write the modified J-integral around the path in Fig. 7b to get

$$\frac{(1-\nu_m^2)K^2}{AE} = \frac{(1-c)(1-\nu_m^2)K_m^2}{E_m} + V[\sigma(L)] \tag{18}$$

where the constant A takes into account the orthotropy of the composite, and, as before, the (1-c) factor reflects the fact that fibers interrupt the crack front. Note that the first term on the right is the same as $(1-c)G_m$. If we now assert that the bridged configuration propagates steadily, with simultaneous matrix fracture and "last" fiber failure, we can set $\sigma(L)$ equal to cS, where S is the fiber strength. Now define the modified toughening ratio

$$\Lambda \equiv \frac{K/K_m}{\sqrt{(1-c)AE/E_m}} \tag{19}$$

and use the formulas (16) for V in (18). Then we get

$$\Lambda = \left[1 + \left(\frac{cS}{\sigma_1}\right)^2 \left(\frac{\sigma_1}{\sigma_0}\right)^2 \right]^{1/2} \qquad \text{for} \quad \frac{cS}{\sigma_1} \le \frac{1}{3}\left(\frac{\sigma_1}{\sigma_0}\right)^2 \tag{20a}$$

$$= \left[1 + 2\left(\frac{cS}{\sigma_1}\right)^3 + \frac{1}{27}\left(\frac{\sigma_1}{\sigma_0}\right)^6 \right]^{1/2} \qquad \text{for} \quad \frac{cS}{\sigma_1} \ge \frac{1}{3}\left(\frac{\sigma_1}{\sigma_0}\right)^2 \tag{20b}$$

and this gives the curves in Fig. 8, showing Λ vs. cS/σ_1 for $\sigma_1/\sigma_0 = 0,1,2$. An estimate for the orthotropy factor A in the definition (19) of the modified toughening ratio Λ is given in Appendix A.

These results may be rewritten to show Λ as a function of (cS/σ_{cr}) in the form

$$\Lambda = \left[1 + \left(\frac{cS}{\sigma_{cr}}\right)^2 \left(\frac{\sigma_{cr}}{\sigma_0}\right)^2 \right]^{1/2} \qquad \text{for} \quad \frac{cS}{\sigma_{cr}} \le \frac{(\sigma_1/\sigma_0)^3}{3(\sigma_{cr}/\sigma_0)} \tag{21a}$$

$$= \left[1 + 2\frac{\left(\frac{cS}{\sigma_{cr}}\right)^3 \left(\frac{\sigma_{cr}}{\sigma_0}\right)^3}{\left(\frac{\sigma_1}{\sigma_0}\right)^3} + \frac{1}{27}\left(\frac{\sigma_1}{\sigma_0}\right)^6 \right]^{1/2} \qquad \text{for} \quad \frac{cS}{\sigma_{cr}} \ge \frac{(\sigma_1/\sigma_0)^3}{3(\sigma_{cr}/\sigma_0)} \tag{21b}$$

wherein (σ_{cr}/σ_0), given in Fig. 3, in turn depends on σ_1/σ_0. Thus, the toughening has been related directly to the ratio of the fiber strength to the theoretical stress for steady-state matrix cracking. Curves showing Λ vs. cS/σ_{cr} for $(\sigma_1/\sigma_0)^3 = 0, 1, 2, 3$, and ∞ are given in Fig. 9. Recall that in the case of steady-state matrix cracking, the post-cracking strength σ_{max} of the composite is approximately equal to cS, assuming $cS > \sigma_{cr}$. Accordingly, the abscissa in Fig. 9 may be interpreted as σ_{max}/σ_{cr} for $cS/\sigma_{cr} > 1$.

In the limiting case $\sigma_1/\sigma_0 \to \infty$, $\sigma_{cr} = \sigma_0$, and the modified toughening ratio is simply

$$\Lambda = \left[1 + \left(\frac{cS}{\sigma_0}\right)^2 \right]^{1/2} \tag{22}$$

(For all finite $\sigma_1/\sigma_0 > 3^{1/3}$, we still have $\sigma_{cr} = \sigma_0$, but then (22) holds only for $cS/\sigma_0 < (\sigma_1/\sigma_0)^3/3$; for larger values of cS/σ_0 frictional sliding will occur before fracture, even if it is absent during steady matrix cracking.)

For $\sigma_1/\sigma_0 \to 0$, in which case $\sigma_{cr} \approx \sigma_1$, we have

$$\Lambda \approx \left[1 + 2\left(\frac{cS}{\sigma_1}\right)^3 \right]^{1/2}. \tag{23}$$

Fig. 8 shows that this approximation remains quite accurate for moderately high values of σ_1/σ_0.

Note that Figs. 3 and 9 show that for decreasing frictional resistance τ, and hence lower σ_1, the steady-state matrix-cracking stress σ_{cr} goes down, but the fracture toughness increases. The curves in Fig. 9 would appear to imply an inherent limitation on the amount of toughening that could reasonably be expected from a well-designed composite. Fracture toughness is an increasing function of the ratio σ_{max}/σ_{cr} associated with matrix cracking and failure in uniaxial tension. Since it is unlikely that values much larger than 2 for this ratio would be considered desirable, toughening ratios around 4 may be the most one might seek.

TOUGHENING VS. BRIDGE LENGTH; RESISTANCE CURVES

To calculate the size of the bridged zone when fracture occurs we have to set up and solve an integral equation for the stress in the intact fibers along the crack faces. For this purpose we contemplate the spring model of Fig. 7a, and note that the crack opening displacement v(x) is given by

$$v(x) = \frac{4(1-\nu_m^2)K}{\sqrt{2\pi}AE}\sqrt{x} - \frac{4(1-\nu_m^2)}{\pi AE}\int_0^L \sigma(x)\log\left(\frac{\sqrt{x}+\sqrt{x'}}{\sqrt{|x-x'|}}\right)dx' \tag{24}$$

where the first term represents the displacement due to the far-field loading, and the second term is the crack-closing effect of the spring stresses. The orthotropy factor A, the same one that appears in the J-integral (18), correctly modifies standard formulas for crack-face displacement in isotropic materials (e.g. TADA et al., 1985). Equating the displacements in the bridged zone to those given by the constitutive relations (17) found for the springs provides the integral equation

$$\frac{4(1-\nu_m^2)K}{\sqrt{2\pi}AE}\sqrt{x} - \frac{4(1-\nu_m^2)}{\pi AE}\int_0^L \sigma(x)\log\left(\frac{\sqrt{x}+\sqrt{x'}}{\sqrt{|x-x'|}}\right)dx'$$

$$= \frac{(1-c)(1-\nu_m^2)K_m^2}{\sigma_0^2 E_m}\sigma(x) \qquad \text{for } \frac{\sigma(x)}{\sigma_0} \le \frac{1}{3}\left(\frac{\sigma_1}{\sigma_0}\right)^3$$

$$= \frac{(1-c)(1-\nu_m^2)K_m^2}{E_m}\left[\frac{3}{2}\frac{\sigma^2(x)}{\sigma_1^3} + \frac{1}{6}\frac{\sigma_1^3}{\sigma_0^4}\right] \qquad \text{for } \frac{\sigma(x)}{\sigma_0} \ge \frac{1}{3}\left(\frac{\sigma_1}{\sigma_0}\right)^3. \tag{25}$$

It is shown in Appendix B how this integral equation, suitably non-dimensionalized, was solved simultaneously with the J-integral relation (18) to provide results for the modified toughening ratio Λ as a function of the non-dimensional bridge length

$$\alpha = \frac{4}{\pi}\frac{E_m}{AE(1-c)}\left(\frac{\sigma_{cr}}{K_m}\right)^2 L. \tag{26}$$

Fig. 10 shows curves thereby calculated for Λ vs. α, for $(\sigma_1/\sigma_0)^3 = 0, 2, \infty$. Remarkably, the introduction of the theoretical steady-state matrix-cracking stress σ_{cr} into the definition (26) for the non-dimensional bridge length has made the results come out nearly the same over the full range of composite parameters.

With Λ given by Eq. (21) (or Fig. 9), these results provide the bridge length L corresponding to propagation of the cracked configuration of Fig. 1, with simultaneous matrix fracture and fiber failure at the end of the bridged zone. However, the curves of Fig. 10 have another interpretation as *resistance curves* , in the following sense. Suppose a pre-existent, unbridged crack in the composite, cutting through both fibers and matrix, is subjected to a gradually increasing far-field K, and re-define Λ in Fig. 10 in terms of this current value of K. As K increases, the crack will advance into the matrix material, and crack-bridging fibers will remain intact as long as Λ remains below its critical value for final fracture of the composite. If we now redefine L as the amount of matrix crack growth that occurs before overall composite fracture, the relation between the current values of K and L is given by the curves of Fig. 10.

It is noteworthy that reduction of the frictional resistance τ , and hence σ_{cr}, will result in increased matrix cracking and bridge lengths before and at final fracture .

CONCLUDING REMARKS

The fracture toughness of brittle materials reinforced by aligned brittle fibers has been related simply to parameters associated with the steady-state matrix cracking of such materials. In each of these processes the fiber-matrix interface shear resistance plays an important role, with opposite effects: decreasing shear strength increases the toughness but lowers the matrix cracking resistance. This is consistent with the fact that low interface friction may result in large amounts of matrix cracking associated with the fracture resistance curves of the composite. The effects of various other physical and geometrical parameters may be assessed with the help of the formulas and curves that have been presented.

ACKNOWLEDGEMENTS

This work was initiated by the DARPA Materials Research Council under the auspices of the University of Michigan, and was continued with support from the National Science Foundation (Grant MSM-84-16392), the Office of Naval Research (Contract N00014-84-K-0510), DARPA University Research Initiative (Subagreement P. O. #VB38639-0 with the University of California, Santa Barbara, ONR Prime Contract N00014-86-K-0753), and the Division of Applied Sciences, Harvard University.

REFERENCES

BUDIANSKY, B — 1986 — In *Proceedings of the Tenth U. S. National Congress of Applied Mechanics,* Austin, Texas, June 20, 1986 (edited by J. P. Lamb), 25-32.

BUDIANSKY, B., AMAZIGO, J. C. and EVANS, A. G. — 1988 — *J. Mech. Phys. Solids*, in press.

BUDIANSKY, B., HUTCHINSON, J. W. and EVANS, A. G. — 1986 — *J. Mech. Phys. Solids,* **34**,167-189.

HILL, R. — 1965 — *J. Mech. Phys. Solids*, **13**, 189-198.

MARSHALL, D. B. and COX, B. N. — 1987 — *Acta. Metall.*, **35**, 2607-2619.

MARSHALL, D. B. and EVANS, A. G. — 1988 — *Materials Forum,* in press.

MARSHALL, D. B. and EVANS, A. G. — 1986 — In *Fracture Mechanics of Ceramics* (edited by R. C. Bradt, A. G. Evans, D. P. H. Hasselman and F. F, Lange), Vol. 7, 1-15 Plenum Press, New York.

ROSE, L. R. F. — 1987 — *J. Mech. Phys. Solids*, **35**, pp. 383-405.

TADA, H., PARIS, P. C. and IRWIN, G. R. — 1985 — "The Stress Analysis of Cracks Handbook", Del Research, St. Louis, MO.

THOULESS, M. D. and EVANS, A. G. — 1988 — *Acta. Metall.*, in press.

APPENDIX A

ORTHOTROPIC FACTOR A

Consider an orthotropic material, isotropic in planes normal to the x_1-axis. The energy release rate G_I associated with a mode I crack in the x_2-x_3 plane is related to the stress intensity factor K_I by (TADA et al 1985)

$$G_I = \hat{C} K_I^2 \tag{A1}$$

where $\hat{C}$ is defined in terms of compliances A_{ij} by

$$\hat{C} = \sqrt{\frac{A_{11}A_{22}}{2}}\left[\sqrt{\frac{A_{22}}{A_{11}}} + \frac{2A_{12} + A_{66}}{2\,A_{11}}\right]^{1/2} \tag{A2}$$

The compliances may be expressed in terms of conventional elastic constants E, $\bar{E}$, G, ν and $\bar{\nu}$ defined by

$$\varepsilon_1 = \sigma_1/E \ , \ \varepsilon_2 = -\nu\sigma_1/E \qquad \text{for } \sigma_2 = \sigma_3 = 0 \ ;$$

$$\varepsilon_2 = \sigma_2/\bar{E} \ , \ \varepsilon_3 = -\bar{\nu}\sigma_2/\bar{E} \qquad \text{for } \sigma_1 = \sigma_3 = 0 \ ;$$

and

$$\gamma_{12} = \sigma_{12}/G.$$

For plane-strain cracks

$$A_{11} = \frac{1}{E}(1 - \nu^2\bar{E}/E), \ A_{12} = -\frac{\nu}{E}(1 + \bar{\nu}), \ A_{22} = \frac{1}{\bar{E}}(1 - \bar{\nu}^2), \ A_{66} = \frac{1}{G} \tag{A3}$$

In the J-integral expression (18) $\hat{C}$ is represented by $(1-\nu_m^2)/AE_m$ and therefore

$$A = \frac{1 - \nu_m^2}{\hat{C}E_m} \tag{A4}$$

For aligned fibers the elastic constants E, $\bar{E}$, G, ν and $\bar{\nu}$ may be estimated on the basis of the self-consistent model (HILL, 1965) in terms of E_m, E_f, ν_m, ν_f and c. For $\nu_f = \nu_m = 1/4$, the consequent dependence of A on c is plotted for various values of $E_f/E_m > 1$ in Figure 11.

APPENDIX B

INTEGRAL EQUATION SOLUTION

The substitutions

$$\Lambda = \frac{K/K_m}{\sqrt{(1-c)AE/E_m}}, \qquad g = \frac{1}{\Lambda\sqrt{2}}\frac{\sigma}{\sigma_{cr}} \tag{B1a}$$

$$s = \frac{4}{\pi}\frac{E_m}{AE(1-c)}\left(\frac{\sigma_{cr}}{K_m}\right)^2 x, \qquad \alpha = \frac{4}{\pi}\frac{E_m}{AE(1-c)}\left(\frac{\sigma_{cr}}{K_m}\right)^2 L \tag{B1b}$$

into the integral equation (25) give

$$\sqrt{s} - \int_0^\alpha g(t)\log\left(\frac{\sqrt{s}+\sqrt{t}}{\sqrt{|s-t|}}\right)dt = \mu^2 g(s), \qquad g(s) \le \frac{r^3}{3\sqrt{2}\Lambda\mu} \tag{B2a}$$

$$= \frac{3}{2}\left(\frac{\mu}{r}\right)^3 \Lambda\sqrt{2}\, g^2(s) + \frac{\mu r^3}{6\sqrt{2}\Lambda}, \quad \text{otherwise} \tag{B2b}$$

where

$$r = \sigma_1/\sigma_0, \quad \mu = \sigma_{cr}/\sigma_0.$$

Making the same substitutions (B1) into (18) gives

$$\Lambda^2 - 1 = 2\mu^2\Lambda^2 g^2(\alpha), \qquad g(\alpha) \le \frac{r^3}{3\sqrt{2}\Lambda\mu} \tag{B3a}$$

$$= 4\sqrt{2}\left(\frac{\mu}{r}\right)^3 \Lambda^3 g^3(\alpha) + \frac{r^6}{27}, \qquad g(\alpha) \ge \frac{r^3}{3\sqrt{2}\Lambda\mu} \tag{B3b}$$

An alternative expression for Λ that can be shown to be consistent with (18) and the integral equation (25) follows from the relation (TADA et al, 1985)

$$\sqrt{1-c}\, K_m = K - \sqrt{\frac{2}{\pi}}\int_0^L \frac{\sigma(x)}{x}\,dx,$$

namely,

$$\Lambda = \left[1 - \int_0^\alpha \frac{g(s)}{\sqrt{s}}\,ds\right]^{-1}. \tag{B4}$$

The solution of the integral equation (B2) follows the set-up developed in BUDIANSKY, AMAZIGO, and EVANS (1988). Differentiate the equation with respect to s to get

$$\frac{1}{2\sqrt{s}} - \frac{1}{2}\int_0^{\alpha} \sqrt{\frac{t}{s}}\,\frac{g(t)}{t-s}\,dt = \mu^2\, g'(s), \qquad s \le s_0 \tag{B5a}$$

$$= \frac{3\sqrt{2}\Lambda}{r^3}\,\mu^3\, g(s)\, g'(s), \qquad s \ge s_0 \tag{B5b}$$

where s_0 satisfies

$$g(s_0) = \frac{r^3}{3\sqrt{2}\Lambda\mu}. \tag{B6}$$

To satisfy the original equation (B2) we have to enforce it at one point in addition to satisfying (B5) for s in $(0,\alpha)$. Enforcing the integral equation at $s = \alpha$ gives

$$\sqrt{\alpha} - \int_0^{\alpha} g(t)\log\left(\frac{\sqrt{\alpha}+\sqrt{t}}{\sqrt{\alpha-t}}\right)dt = \frac{3}{2}\left(\frac{\mu}{r}\right)^3 \Lambda\sqrt{2}\, g^2(\alpha) + \frac{\mu r^3}{6\sqrt{2}\Lambda}. \tag{B7}$$

We now let

$$g(s) = \frac{H(s)}{\sqrt{s}} \tag{B8}$$

in (B5) to obtain

$$s^{3/2} - s^{3/2}\int_0^{\alpha} \frac{H(t)}{t-s}\,dt = \mu^2\sqrt{s}\,[2sH'(s) - H(s)], \qquad s \le s_0 \tag{B9a}$$

$$= \frac{3\sqrt{2}\Lambda}{r^3}\,\mu^3\, H(s)\,[2sH'(s) - H(s)], \qquad s \ge s_0. \tag{B9b}$$

It is convenient to write

$$H(s) = C(s/\alpha) + f(s) \tag{B10}$$

where $C = \sqrt{\alpha}\,g(\alpha)$, and $f(0) = f(\alpha) = 0$. Then

$$s^{3/2}\left(1-\int_0^{\alpha}\frac{f(t)}{t-s}\,dt\right)+C\,s^{3/2}\left[\frac{s}{\alpha}\log\frac{\alpha-s}{s}-1\right]$$

$$=\begin{cases}\mu^2\sqrt{s}\left[\frac{s}{\alpha}C+2sf'(s)-f(s)\right], & s\le s_0 \qquad \text{(B11a)}\\[2ex] 3\sqrt{2}\Lambda\left(\frac{\mu}{r}\right)^3\left[\left(\frac{s}{\alpha}\right)^2 C\{C+2\alpha f'(s)\}+f\{2sf'(s)-f(s)\}\right], & s\ge s_0 \qquad \text{(B11b)}\end{cases}$$

Now let

$$s=\frac{\alpha}{2}(1-\cos\theta) \tag{B12}$$

and expand f in the Fourier series

$$f(s)=\sum_1^N a_n\sin(n\theta). \tag{B13}$$

We note that

$$\int_0^{\alpha}\frac{f(t)}{t-s}\,dt=\pi\sum_1^N a_n\cos(n\theta).$$

We now substitute the above into (B11), multiply the resulting equation by $\sin(m\theta)$ and integrate over $[0,\alpha]$ to get

$$B_m(\theta_0)\,C+3\sqrt{2}\Lambda\left(\frac{\mu}{r}\right)^3 D_m(\theta_0)\,C^2+\sum_{n=1}^N E_{mn}(\theta_0)\,a_n+3\sqrt{2}\Lambda\left(\frac{\mu}{r}\right)^3 C\sum_{n=1}^N nF_{mn}(\theta_0)\,a_n$$

$$+3\sqrt{2}\Lambda\left(\frac{\mu}{r}\right)^3\sum_{n=1}^N\sum_{j=1}^N G_{mnj}(\theta_0)\,a_n a_j=\alpha^{3/2}A_m,\qquad m=1,..,N \tag{B14}$$

where

$$B_m(\theta_0)=\alpha^{3/2}(A_m+Q_m)+\sqrt{\alpha}\,\mu^2 H_m(\theta_0),$$

$$E_{mn}(\theta_0)=\alpha^{3/2}\pi K_{mn}+2\mu^2\sqrt{\alpha}\,m\,L_{mn}(\theta_0)-\mu^2\sqrt{\alpha}\,U_{mn}(\theta_0),$$

$$\begin{aligned}G_{mnj}(\theta_0)&=n[S_{n+j,m}(\theta_0)+\mathrm{sign}(j-n)\,S_{|j-n|,m}(\theta_0)]-T_{njm}(\theta_0), && n\ne j\\ &=2S_{2n,m}(\theta_0)-T_{nnm}(\theta_0), && n=j\end{aligned}$$

$$A_m = m(-1)^{m+1}\left(\frac{3}{4m^2-1} + \frac{1}{4m^2-9}\right),$$

$$D_1 = \frac{11}{24} + \frac{5}{16}\cos\theta_0 - \frac{1}{8}\cos 2\theta_0 + \frac{1}{48}\cos 3\theta_0,$$

$$D_2 = -\frac{103}{192} - \frac{1}{4}\cos\theta_0 + \frac{3}{16}\cos 2\theta_0 - \frac{1}{12}\cos 3\theta_0 + \frac{1}{64}\cos 4\theta_0,$$

$$D_m = (-1)^{m+1}\left[\frac{3}{8m} + \frac{1}{2}\frac{m}{m^2-1} + \frac{1}{8}\frac{m}{m^2-4}\right] - \frac{1}{4}\left[\frac{\cos(m+1)\theta_0}{m+1} + \frac{\cos(m-1)\theta_0}{m-1}\right]$$

$$+\frac{3}{8m}\cos m\theta_0 + \frac{1}{16}\left[\frac{\cos(m+2)\theta_0}{m+2} + \frac{\cos(m-2)\theta_0}{m-2}\right], \qquad m > 2$$

$$F_{mn} = \begin{cases} \frac{1}{2}\left(V_{n+m} + \operatorname{sign}(m-n)\, V_{|n-m|}\right), & \text{for } m \neq n \\ \frac{1}{2} V_{2n}, & \text{for } m = n \end{cases}$$

$$H_m = -\frac{3}{8}\left[\frac{\sin(m+1/2)\theta_0}{m+1/2} - \frac{\sin(m-1/2)\theta_0}{m-1/2}\right] + \frac{1}{8}\left[\frac{\sin(m+3/2)\theta_0}{m+3/2} - \frac{\sin(m-3/2)\theta_0}{m-3/2}\right],$$

$$K_{mn} = \frac{m(-1)^{m+n}}{8}\left[\frac{3}{(n+1/2)^2-m^2} + \frac{3}{(n-1/2)^2-m^2} + \frac{1}{(n+3/2)^2-m^2} + \frac{1}{(n-3/2)^2-m^2}\right],$$

$$S_{k,j} = \frac{1}{2}\left(R_{|k-j|} - R_{k+j}\right),$$

$$T_{njm} = \frac{1}{4}\left(\frac{\cos(n+j-m)\theta_0}{n+j-m} + \frac{\cos(j+m-n)\theta_0}{j+m-n} + \frac{\cos(m+n-j)\theta_0}{m+n-j} - \frac{\cos(n+j+m)\theta_0}{n+j+m}\right)$$

$$+\frac{2njm(-1)^{n+j+m}}{n^4+j^4+m^4-2(n^2j^2+j^2m^2+m^2n^2)}, \quad \text{for } n \neq j+m \text{ or } j \neq n+m \text{ or } m \neq j+n$$

$$= \frac{1}{8}\left[\frac{\cos(2j\theta_0)}{j} + \frac{\cos(2n\theta_0)}{n} - \frac{\cos(2m\theta_0)}{m}\right] - \frac{1}{8}\left(\frac{1}{j} + \frac{1}{n} - \frac{1}{m}\right), \qquad m = j+n$$

and similar expressions for $n = j + m$ and $j = n + m$ obtained by cyclic permutation of j, n and m.

$$U_{mn} = \frac{1}{4}\left\{ \frac{1}{(m+n)^2-1/4} - \frac{1}{(m-n)^2-1/4} - \frac{\cos\,(m-n+1/2)\theta_0}{m-n+1/2} + \frac{\cos\,(m-n-1/2)\theta_0}{m-n-1/2} \right.$$

$$\left. + \frac{\cos\,(m+n+1/2)\theta_0}{m+n+1/2} - \frac{\cos\,(m+n-1/2)\theta_0}{m+n-1/2} \right\},$$

and

$$L_{mn} = \int_0^{\theta_0} \sin\,(\theta/2)\tan\,(\theta/2)\cos\,(n\theta)\sin\,(m\theta)\,d\theta,$$

$$Q_m = \int_0^{\pi} \sin^5(\theta/2)\log\left(\frac{1+\cos\theta}{1-\cos\theta}\right)\sin\,(m\theta)\,d\theta,$$

$$R_n = \int_{\theta_0}^{\pi} \frac{1-\cos\theta}{\sin\theta}\,[\cos\,(n\theta) - (-1)^n]\,d\theta,$$

$$V_k = \int_{\theta_0}^{\pi} \frac{(1-\cos\theta)^2}{\sin\theta}\sin\,(k\theta)\,d\theta,$$

were evaluated numerically in spite of the fact that the last two integrals can be evaluated analytically in terms of finite series. θ_0 satisfies the equation (B6) with $s_0 = (\alpha/2)(1 - \cos\theta_0)$, that is

$$\frac{1}{2}(1-\cos\theta_0)\,C + \sum_{n=1}^{N} a_n \sin(n\theta_0) - \frac{r^3\sqrt{\alpha}}{3\sqrt{2}\Lambda\mu}\sin\,(\theta_0/2) = 0. \qquad \text{(B15)}$$

Substitution for g into (B7) using (B8), (B10), (B12) and (B13) gives

$$\frac{1}{3}(1+2\log 2)\,C + \frac{3\Lambda}{\sqrt{2}}\left(\frac{\mu}{r}\right)^3\alpha^{-3/2}C^2 + \sum_{n=1}^{N} P_n a_n = 1 - \frac{\mu r^3}{6\sqrt{2}\Lambda}\alpha^{-1/2}, \qquad \text{(B16)}$$

where
$$P_n = \int_0^{\pi} \cos\,(\theta/2)\log\frac{1+\sin\,(\theta/2)}{\cos\,(\theta/2)}\sin\,(n\theta)\,d\theta$$

Equation (B3) relating C and Λ is

$$\Lambda^2 - 1 = 2\mu^2\alpha^{-1}(\Lambda C)^2, \qquad \Lambda C \le r^3\sqrt{\alpha}/3\sqrt{2}\mu \qquad \text{(B17a)}$$

$$= 4\sqrt{2}(\mu/r)^3\alpha^{-3/2}(\Lambda C)^3 + r^6/27, \qquad \Lambda C \ge r^3\sqrt{\alpha}/3\sqrt{2}\mu \qquad \text{(B17b)}$$

while the alternative formula (B4) becomes

$$\Lambda = \left[1 - C - \pi \sum_{1}^{N} a_n \right]^{-1} . \tag{B18}$$

For prescribed values of $r = \sigma_1/\sigma_0$ and α the N+3 nonlinear equations (B14), (B15), (B16) and (B17) were solved by the Newton-Raphson iteration method for the N+3 unknowns C, a_n, $n=1,..,N$, Λ and θ_0. The formula (B18) provided a check on the accuracy of the numerical scheme. For values of α presented in Fig. 10 the error in the value of Λ was less than 1%. For $\sigma_1/\sigma_0 \to \infty$, $\mu \to 1$ and equation (B2) becomes

$$\sqrt{s} - \int_0^{\alpha} g(t) \log \frac{\sqrt{s} + \sqrt{t}}{\sqrt{|s-t|}} \, dt = g(s).$$

This is equivalent to the linear spring problem analyzed fully by BUDIANSKY, AMAZIGO, and EVANS (1988) and ROSE (1987).

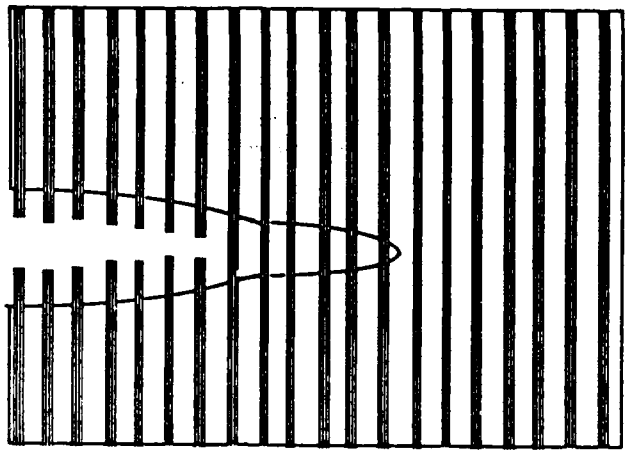

Fig. 1 Composite fracture; crack-bridging by aligned fibers in vicinity of crack tip.

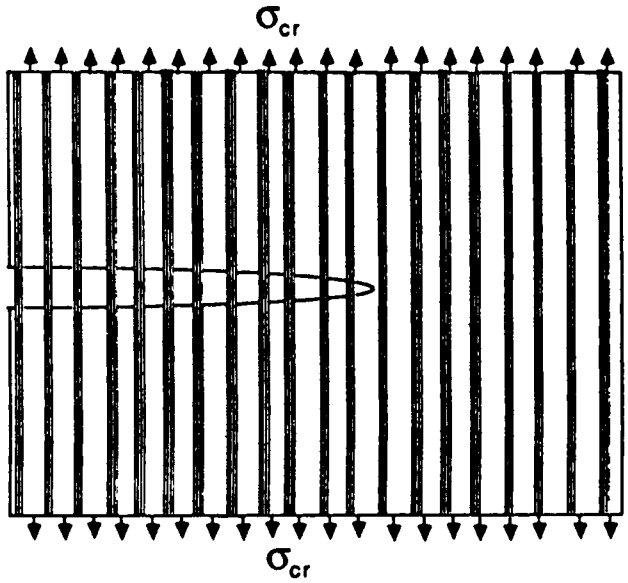

Fig. 2 Steady-state matrix cracking; intact fibers.

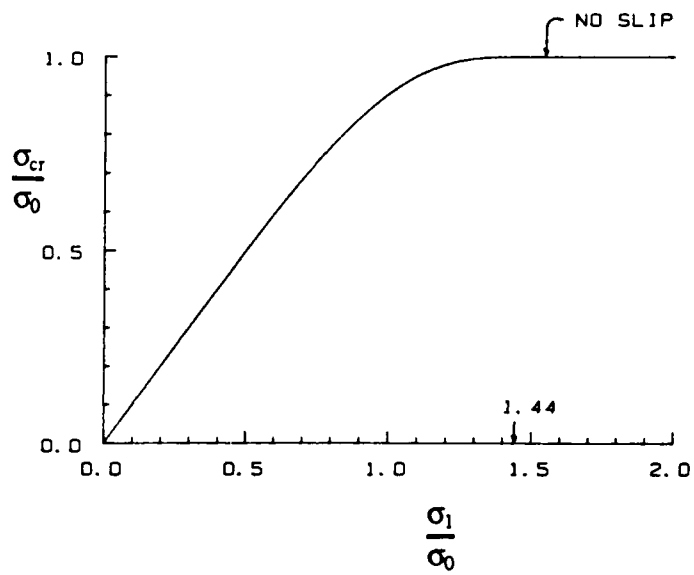

Fig. 3 Theoretical results for matrix cracking stress σ_{cr}.

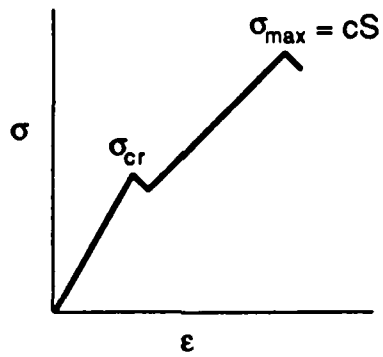

Fig. 4 Idealized stress-strain curve for aligned-fiber composite; matrix cracking at $\sigma \sim \sigma_{cr}$; failure at $\sigma \sim \sigma_{max} = cS$.

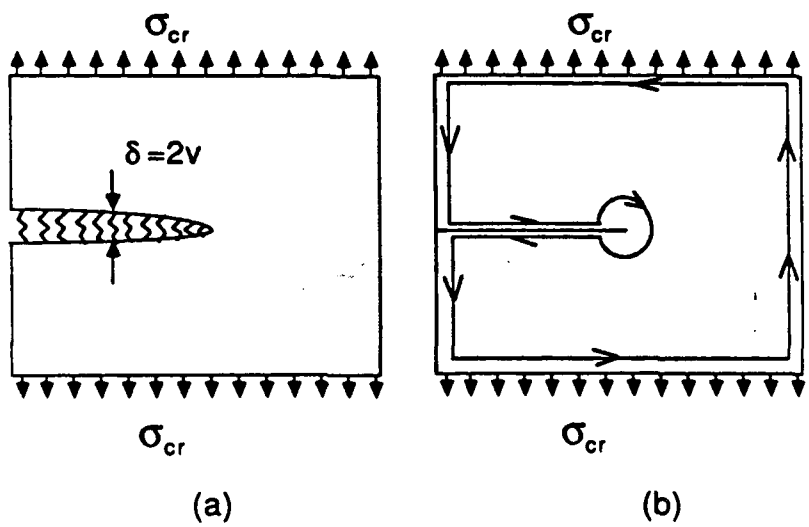

Fig. 5 (a) Spring model, steady matrix cracking.
(b) J-integral path.

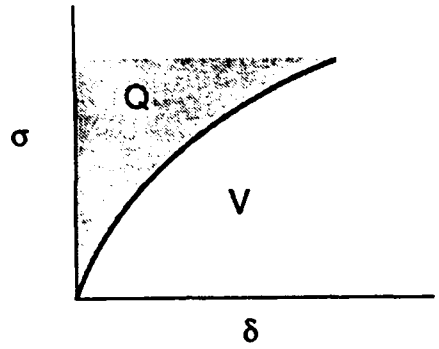

Fig. 6 Spring stress-stretch relation; V = strain energy; Q = complementary energy.

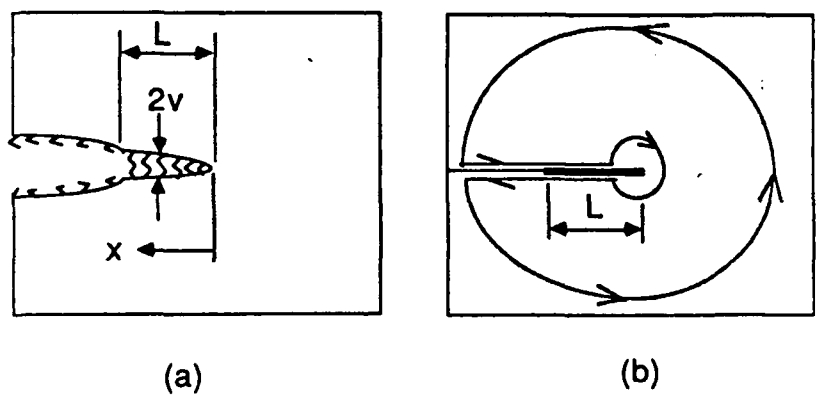

Fig. 7 (a) Spring model; composite fracture.
(b) J-integral path.

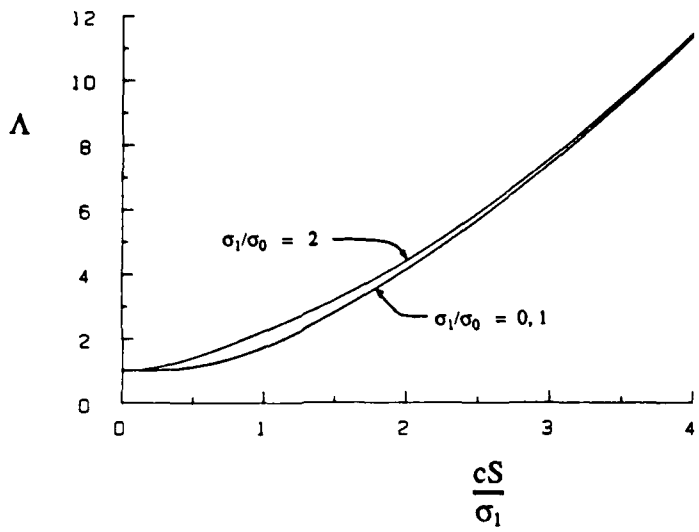

Fig. 8 Modified toughening ratio $\Lambda = \dfrac{K/K_m}{\sqrt{(1-c)AE/E_m}}$; abscissa $\approx \sigma_{max}/\sigma_1$ for $cS > \sigma_{cr}$.

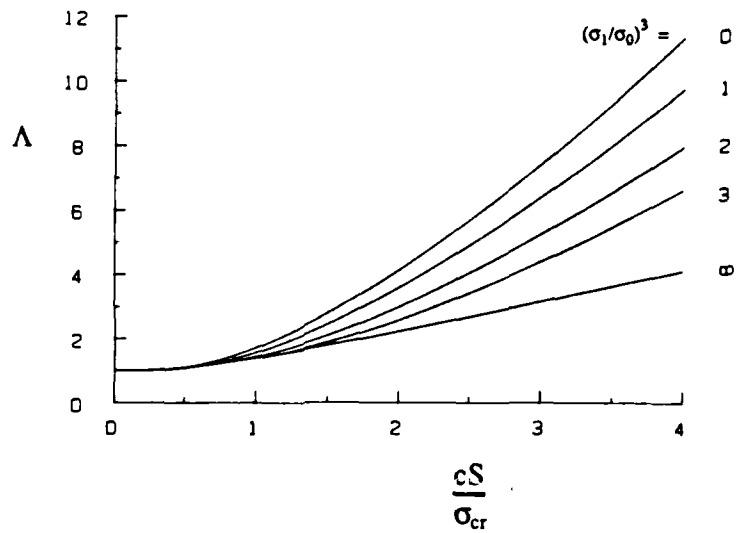

Fig. 9 Modified toughening ratio $\Lambda = \dfrac{K/K_m}{\sqrt{(1-c)AE/E_m}}$; abscissa $\approx \sigma_{max}/\sigma_{cr}$ for $cS > \sigma_{cr}$.

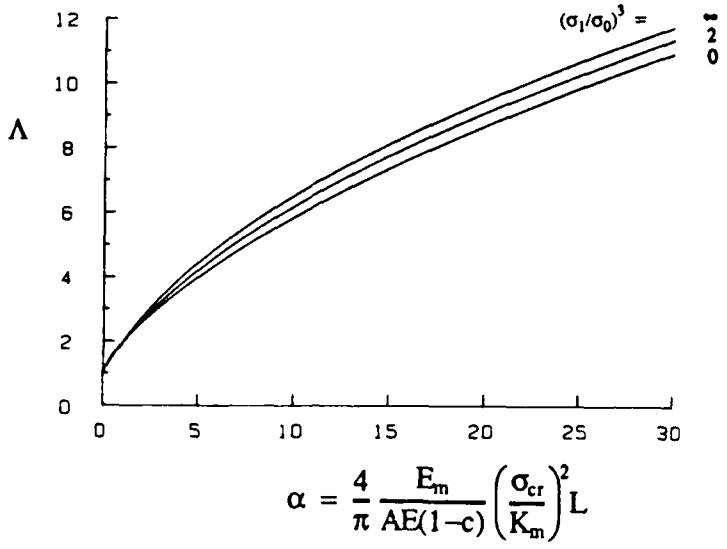

Fig. 10 Modified toughening ratio $\Lambda = \dfrac{K/K_m}{\sqrt{(1-c)AE/E_m}}$ vs. non-dimensional bridge length; also resistance curves.

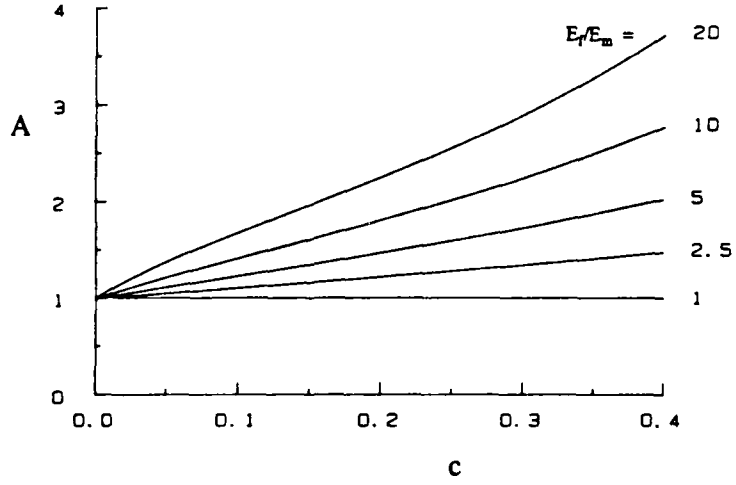

Fig. 11 Orthotropy factor A vs. fiber concentration c; $\nu_f = \nu_m = 1/4$.